PLOS ONE

RESEARCH ARTICLE

Gnaz couples the circadian and dopaminergic system to G protein-mediated signaling in mouse photoreceptors

Patrick Vancura[1]*, Shaima Abdelhadi[1], Erika Csicsely[1], Kenkichi Baba[2], Gianluca Tosini[2], P. Michael Iuvone[3], Rainer Spessert[1]

1 Institute of Functional and Clinical Anatomy, University Medical Center of the Johannes Gutenberg University, Mainz, Germany, **2** Neuroscience Institute and Department of Pharmacology and Toxicology, Morehouse School of Medicine, Atlanta, Georgia, United States of America, **3** Department of Ophthalmology, Emory University School of Medicine, Atlanta, Georgia, United States of America

* p.vancura@uni-mainz.de

Citation: Vancura P, Abdelhadi S, Csicsely E, Baba K, Tosini G, Iuvone PM, et al. (2017) *Gnaz* couples the circadian and dopaminergic system to G protein-mediated signaling in mouse photoreceptors. PLoS ONE 12(10): e0187411. https://doi.org/10.1371/journal.pone.0187411

Editor: Nicolas Cermakian, McGill University, CANADA

Received: August 23, 2017

Accepted: October 19, 2017

Published: October 31, 2017

Data Availability Statement: All relevant data are within the paper.

Funding: This research was funded in part by grants from the National Institutes of Health: R01EY026291 to GT, R01EY004864 to PMI, P30EY006360 to PMI, and R01EY02711 to PMI.

Competing interests: Gianluca Tosini is a member of PLOS ONE Editorial board. This does not alter the authors' adherence to PLOS ONE policies on sharing data and materials.

Abstract

The mammalian retina harbors a circadian clockwork that regulates vision and promotes healthiness of retinal neurons, mainly through directing the rhythmic release of the neurohormones dopamine—acting on dopamine D_4 receptors—and melatonin—acting on MT_1 and MT_2 receptors. The gene *Gnaz*—a unique Gi/o subfamily member—was seen in the present study to be expressed in photoreceptors where its protein product $G\alpha_z$ shows a daily rhythm in its subcellular localization. Apart from subcellular localization, *Gnaz* displays a daily rhythm in expression—with peak values at night—in preparations of the whole retina, microdissected photoreceptors and photoreceptor-related pinealocytes. In retina, *Gnaz* rhythmicity was observed to persist under constant darkness and to be abolished in retina deficient for *Clock* or dopamine D_4 receptors. Furthermore, circadian regulation of *Gnaz* was disturbed in the *db*/*db* mouse, a model of diabetic retinopathy. The data of the present study suggest that *Gnaz* links the circadian clockwork—via dopamine acting on D_4 receptors—to G protein-mediated signaling in intact but not diabetic retina.

Introduction

The mammalian retina is known to harbor an intrinsic circadian clock system [1, 2] where circadian clocks are localized in various types of retinal neurons including horizontal cells, amacrine cells [3, 4] and photoreceptors [5–7]. The molecular clock enables the retina to adjust its physiology to adapt to daily changes in environmental demands. In particular, the retinal clock promotes adjustment of visual processing [8] that manifests in circadian changes in the retinal electrical responses to light, which can be measured using the ERG [9, 10]. Clock-dependent regulation of retinal physiology involves the neurohormones melatonin and dopamine [11, 12]. Both neurohormones play opposing roles in retinal adaptation. While melatonin by acting on MT_1 and MT_2 receptors promotes adaptation to darkness [13, 14] dopamine supports adaptation to light by acting on D_4 receptors [15–18].

Heterotrimeric G proteins mediate the stimulation of G protein coupled receptors (GPCRs) to regulate a broad range of physiological functions in various tissues [19]. Each G protein consists of an α-subunit that binds and hydrolyzes GTP, as well as a β- and a γ-subunit. Sixteen types of α-subunits, five types of β-subunits and thirteen types of γ-subunits are known in humans. The sixteen α-subunits are encoded by a gene superfamily that can be subdivided into four different classes: *Gnai*, *Gnas*, *Gnaq* and *Gna12/13*. The *Gnai* class encompasses the four families *Gnai*, *Gnaz*, *Gnao* and *Gnat*. Based on their sequence similarities the *Gnaz* family—consisting of exclusively the gene *Gnaz*—and the *Gnat* family—involving the genes *Gnat1* and *Gnat2*—are considered α-transducins. However, *Gnaz* has no function in vision–and for this reason is referred to as *non-visual* α-transducin while *Gnat1* and *Gnat2* are involved in phototransduction and therefore are referred to as *visual* α-transducins.

The transcription of α-transducin display a 24-h rhythm in the rodent retina [20–22]. However, it is an open question whether the α-transducin investigated refers to the non-visual α-transducin *Gnaz* and/or the visual α-transducins *Gnat1* and/or *Gnat2*. The aim of the present study was to investigate (1) as to what extent expression of *Gnaz*, *Gnat1* and/or *Gnat2* is under daily regulation in retina, photoreceptors and photoreceptor-related pinealocytes, (2) depends on a circadian clock, (3) is regulated by the neurohormones melatonin and dopamine and (4) is disturbed in diabetic retinopathy.

Material and methods

Animals

Adult (age of 10–12 weeks) male and female mice (see below) not carrying *rd* mutations and, when indicated, rats (Sprague Dawley) were used in this study. With the exception of the mouse model for diabetic retinopathy (C57BL/6Jb db/+, C57BL/6Jb db/db), the mice used were melatonin-proficient (C3H/$f^{+/+}$, C3H/$f^{+/+}$Clock$^{+/+}$, C3H/$f^{+/+}$Clock$^{-/-}$, C3H/$f^{+/+}$MT1$^{+/+}$, C3H/$f^{+/+}$MT1$^{-/-}$, C3H/$f^{+/+}$Drd4$^{+/+}$ and C3H/$f^{+/+}$Drd4$^{-/-}$). Genotyping was performed by PCR analysis of genomic DNA. C3H/$f^{+/+}$Clock$^{+/+}$ and C3H/$f^{+/+}$Clock$^{-/-}$ were generated by backcrossing Clock mice (strain name: B6.129S4-Clock$^{tm1.1Rep}$/J) obtained from Jackson Laboratory (Bar Harbor, ME, USA) against C3H/$f^{+/+}$ mice for ten generations. Diabetic (*db/db*) and non-diabetic (*db*/+) mice (strain name: BKS.Cq-*Dock7^{m}* +/+ *Lepr^{db}*/J) were purchased from Jackson Laboratory. They were checked for body-weight and blood glucose level by tail vein sampling using Accu-Check Aviva reagent strips (Roche Diagnostics, Mannheim, Germany) at the age of 10 weeks. Diabetic mice displayed enhanced values of blood glucose (397 ± 14 mg/dl) and bodyweight (46 ± 3 g) as compared to non-diabetic mice (blood glucose level: 138 ± 4 mg/dl; bodyweight: 25 ± 1 g).

Animals were kept under light/dark 12:12 (LD) cycles for 3 weeks under standard laboratory conditions (illumination with 200 lux at cage level during the day and dim (< 5 lux) red light during the night, 20 ± 1˚C, water and food ad libitum) and sacrificed at 3-h intervals over a period of 24 hours by decapitation following anesthesia with carbon dioxide. In order to determine putative clock-dependent regulation of genes, mice previously adapted to LD were housed in constant darkness (DD) for one cycle and sacrificed during the next cycle in DD. Animal experimentation was carried out in accordance with the National Institutes of Health Guide on the Care and Use of Laboratory Animals and the ARVO Statement for the Use of Animals in Ophthalmic Vision Research, and approved by the Institutional Animal Care and Use Committees of Morehouse School of Medicine, Emory University, and the European Communities Council Directive (86/609/EEC).

Laser microdissection and pressure catapulting (LMPC)

To prepare the retinae for LMPC, the HOPE technique (DCS, Hamburg, Germany) was applied for fixation [23]. Photoreceptors were isolated from stained sections in a contact- and

contamination-free manner by using the LMPC technique as described previously [6]. The purity grades of the preparations obtained were verified by using a specific gene marker of photoreceptors, namely *Nrl* as a marker for rods [24], and of inner retinal neurons, namely *Th* as a marker for amacrine cells [25]. In comparison to whole retina preparations, in photoreceptors collected by LMPC, the ratio of *Nrl* to *Th* was increased 84-fold.

RNA extraction, reverse transcription (RT) and quantitative polymerase chain reaction (qPCR)

Using the RNeasy Micro Kit (Qiagen, Hilden, Germany) RNA was extracted from the tissue samples as described previously [26]. Subsequently first stranded cDNA was synthesized using the Verso cDNA Kit (Abgene, Hamburg, Germany), following the manufacturer's instructions. Briefly, 4 μl RNA solution was reverse transcribed using anchored oligo-dT primers in a final volume of 20 μl. Following dilution of the obtained cDNA samples in RNase-free water (1:4) quantitative PCR was performed. Quantitative PCR was carried out in a total volume of 20 μL containing 10 μL ABsolute™ QPCR SYBR® Green Fluorescein Mix (Abgene), 0.2 μL of each primer (10 μM), 4.6 μL RNase-free water, and 5 μL sample. Primer sequences are listed in Table 1. PCR amplification and quantification were performed in duplicate using an i-Cycler (BioRad, Munich, Germany) according to the following protocol: denaturation for 30 seconds at 95˚C, followed by 45 cycles of 5 seconds at 95˚C and 30 seconds at 60˚C. By using agarose gel electrophoresis, the generated amplicons for all genes under examination were shown to possess the predicted sizes (Table 1). To further confirm the specificity of the primer sets used—in particular of those for the genes *Gnaz*, *Gnat1* and *Gnat2*—sequencing of the generated amplicons was performed. According to the obtained sequences, the designed primer sets were verified as highly selective to their respective targets. The amount of mRNA in the samples was calculated from the measured threshold cycles (C_t) using an internal standard curve with 10-fold serial dilutions (10^1–10^8 copies/μl). Expression levels of each transcript were normalized with respect to the amount of *Gapdh* mRNA and *18S* rRNA present.

Western blot analysis

For Western blot analysis, samples were loaded on 4–12% NuPAGE Novex Bis-Tris gels (Invitrogen, Carlsbad, CA, USA), separated and then blotted onto PVDF membrane (Westran S, Whatman Inc., Sanford, ME, USA). For immunodetection, membranes were blocked in 5% skim milk and incubated with rabbit polyclonal anti-$G\alpha_z$ antibody (1:500; Santa Cruz Biotechnology, Santa Cruz, USA, sc-388) overnight at 4˚C. Using an ECL detection system (GE Healthcare Amersham, Freiburg, Germany), the horseradish-peroxidase-conjugated secondary antibody (goat anti-rabbit-HRP 1:10.000; Sigma-Aldrich, St. Louis, MO, USA; A0545) was visualized. Monoclonal anti-β-actin HRP-coupled primary antibody (1:40.000; Sigma-Aldrich, St. Louis, MO, USA; A3854) was used to control for equal protein loading. Densitometry measurement was performed using Image Lab 4.1 (Bio-Rad Laboratories, Hercules, CA, USA).

Fluorescence microscopy

Eyes were embedded in optimal cutting temperature (OCT) compound (Tissue-Tek; Sakura Finetek, Tokyo, Japan) and frozen in melting 2-methyl-butane (VWR, Radnor, PA, USA). Cryosections (10 μm) were treated with 0.1% Tween 20 in PBS, washed with PBS and then blocked with antibody diluent containing background reducing components (Dako, Capinteria, CA, USA) for 30 minutes at room temperature. Subsequently sections were incubated with primary antibodies (anti-$G\alpha_z$ polyclonal antibody, 1:100, Santa Cruz Biotechnology, Santa Cruz, USA, sc-388; anti-Centrin3 polyclonal antibody, 1:100, kindly provided by Prof.

Table 1. Primer sequences used for qPCR.

Gene	Accession Number	Primer Sequence 5′ to 3′	Length of PCR Product [bp]
m18S	NR_003278.3	Forward: CAACACGGGAAACCTCAC Reverse: TCGCTCCACCAACTAAGAAC	110
mDrd4	NM_007878.2	Forward: GTTGGACGCCTTTCTTCG Reverse: GTTGAGGGCACTGTTGAC	116
mGapdh	BC082592.1	Forward: CATCCCAGAGCTGAAC Reverse: TCAGATGCCTGCTTCAC	144
mGna11	NM_010301.3	Forward: GCATGACAGAGCCCTAGAG Reverse: ACAGGAGAGGAGCCTAGTG	106
mGna12	NM_010302.2	Forward: TGCAGGAGAACCTGAAAG Reverse: TGGTGTGGATTCGAGATG	149
mGna13	NM_010303.3	Forward: CCGTTGTACCACCACTTC Reverse: GAGCTGCTTCAGGTTGTC	102
mGna14	NM_008137.4	Forward: TCTGAACGACGGAAATGG Reverse: AAACAGGGCTTTGCTCTC	135
mGna15	NM_010304.3	Forward: TGAGCGAGTATGACCAGTG Reverse: CAGGATGTCCGTCTTGTTG	143
mGnai1	NM_010305.1	Forward: CCGCGTATATTCAGTGTC Reverse: CTGCACGTTCTTCGTATC	101
mGnai2	NM_008138.4	Forward: TGTTAGGTGCTGGAGAGTC Reverse: CTGGATGGTGTTGCTGTAG	125
mGnai3	NM_010306.3	Forward: AGCAGGTCCAGGGAATATC Reverse: CTCCACAATGCCTGTAGTC	138
mGnal	NM_010307.3	Forward: TGCTTCACAGTGGGAAATCG Reverse: GATGATACCGCTGGTAAAGTGG	114
mGnao1	NM_010308.3	Forward: GACGTGGTGAGTCGTATG Reverse: TACTCCCGAGATCGGTTG	116
mGnaq	NM_008139.5	Forward: GCCACAGCAGGATTGTTAAG Reverse: TTAAAGGGCAAGGGTGGAAG	120
mGnas	NM_010309.4	Forward: CAAGTTCCAGGTGGACAAAG Reverse: CCCGAATGACCATGTTGTAG	146
mGnat1	NM_008140.2	Forward: TTCGCCACAACGTCTATC Reverse: GTGTTAGGTCCATCGTAGTC	110
mGnat2	NM_008141.3	Forward: GCAGAGTTCCAGCTCAATG Reverse: CTCGATGATGCCTGTTGTC	129
mGnaz	NM_010311.3	Forward: GGTCTACATCCAACGTCAGTTC Reverse: TCTGTCACTGCGTCAAACAC	123
mGnb1	NM_008142.4	Forward: CTGTGGTGGCCTGGATAAC Reverse: CCGGCAACAGGACAGATAAC	112
mGnb2	NM_010312.4	Forward: GATTCCATGTGCCGACAG Reverse: GGTCAAAGAGGCGACAAG	121
mGnb3	NM_013530.1	Forward: CTGGCTGAGCTTGTGTCTG Reverse: CATCCTGCGAGGCACTTAC	142
mGnb4	NM_013531.4	Forward: TACTTCTGTGGCCTTCTC Reverse: CACACCTAAGCAGCTAAC	142
mGnb5	NM_010313.2	Forward: GCTATGCACACCAACTACC Reverse: GCTGTCCACTTTCCACATC	112
mGngt1	NM_010314.2	Forward: AGTCCTAGCTGTCCTGGAAATC Reverse: TGGCGCACGCCTTTAATAC	103
mGngt2	NM_023121.2	Forward: AAGGAGCTGTTGAGGATG Reverse: TCTTCTGGGATGCCTTTG	146
mNrl	NM_008736.3	Forward: GTGGAGGAACGGTCCAGATG Reverse: GAACTGGAGGGCTGGGTTAC	149
mTh	NM_009377.1	Forward: CAGCCCTACCAAGATCAAAC Reverse: GTACGGGTCAAACTTCACAG	129

(*Continued*)

Table 1. (*Continued*)

Gene	Accession Number	Primer Sequence 5′ to 3′	Length of PCR Product [bp]
r18S	NR_046237.1	Forward: GTTGGTGGAGCGATTTGTC Reverse: TCAATCTCGGTGGCTGAAC	136
rDrd4	NM_012944.1	Forward: TGGGCTATGTCAACAGTG Reverse: CATCAGCGGTTCTTTCAG	112
rGapdh	NM_017008.4	Forward: TGACTCTACCCACGGCAAG Reverse: CTGGAAGATGGTGATGGGTT	89
rGnaz	NM_013189.2	Forward: CCGAGTACAAGGGTCAGAAC Reverse: TCGGTGGCACAGGTAAAG	121

https://doi.org/10.1371/journal.pone.0187411.t001

Wolfrum, Institute of Zoology, Johannes Gutenberg University, Mainz, Germany) in antibody diluent overnight at 4˚C. Following removal of the primary antibody, slides were washed with PBS and incubated with Alexa Fluor488 or Alexa Fluor568 conjugated donkey anti-mouse or donkey anti-rabbit secondary antibodies (Molecular Probes, Leiden, The Netherlands) for 1 hour in antibody diluent at room temperature. Cell nuclei were counterstained with DAPI (Thermo Fisher Scientific, Waltham, USA). Negative immunohistochemistry controls were performed in parallel by omission of primary antibodies. After they were washed, sections were cover slipped with fluorescent mounting medium (Dako, Capinteria, CA, USA). Stained retinal sections were examined by Axiophot microscope (Zeiss, Jena, Germany) and images were obtained with a digital imaging system (JVC, Yokohama, Japan).

Statistical analysis

All data are expressed as the mean ± standard error of the mean (SEM) of four (qPCR and Western blot) independent experiments. Transcript levels were calculated relative to average expression of each dataset throughout 24 hours to plot temporal expression. Cosinor analysis was used to evaluate variations among the groups in the 24-h profile and to fit sine-wave curves to the circadian data to mathematically estimate the time of peaking gene expression (acrophase) and to assess the amplitude [27, 28]. The model can be expressed according to the equation: $f(t) = A + B \cos(2\pi (t + C)/T)$ with the f(t) indicating relative expression levels of target genes, t specifying the time of sampling (h), A representing the mean value of the cosine curve (mesor; midline estimating statistic of rhythm), B indicating the amplitude of the curve (half of the sinusoid) and C indicating the acrophase (point of time, when the function f(t) is maximum). T gives the time of the period, which was fixed at 24 hours for this experimental setting. Protein levels were calculated relative to actin immunoreactivity of each dataset throughout 24 hours to plot temporal expression. One-way ANOVA (one way analysis of variance) was used to evaluate variations among the groups in the 24-h profile. Significance of daily regulation was defined by showing a $p < 0.05$.

Results

Gnaz mRNA is under daily regulation in retina and pineal gland

To gain insight into the daily regulation of G protein-dependent signal transduction in the mouse retina, transcript levels of different Gα subunits were determined as a function of time-of-day. Among the Gα subunits tested, exclusively the *non-visual* α-transducin gene *Gnaz* displayed a daily rhythm (Fig 1, blue lines; for statistical analysis, see Table 2). Neither of the *visual* α-transducins, *Gnat1* and *Gnat2* (Fig 1, blue lines; for statistical analysis, see Table 2), nor any of the other Gα subunits tested (*Gna11*, *Gna12*, *Gna13*, *Gnal4*, *Gnal5*, *Gnai1*, *Gnai2*,

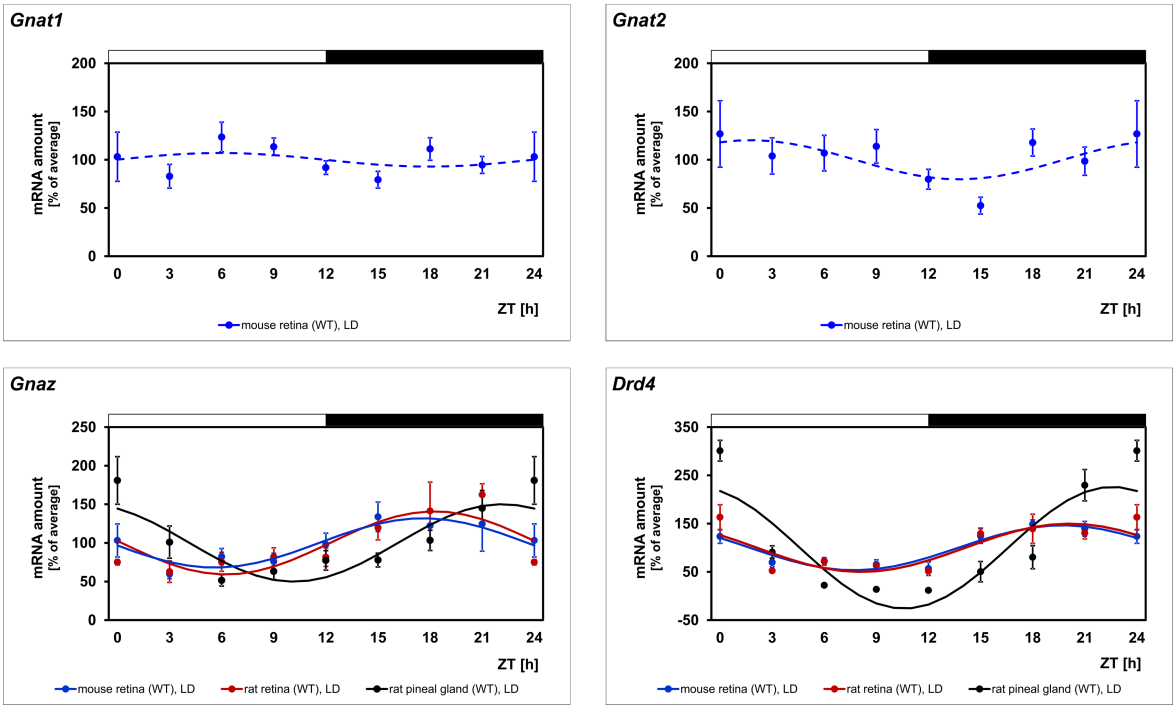

Fig 1. Daily profiling of the different types of α-transducins to be under daily regulation. Transcript levels of the non-visual α-transducin *Gnaz*, the visual α-transducins *Gnat1* and *Gnat2*, and the gene encoding the dopamine D_4 receptor, *Drd4*, were measured using qPCR under LD in mouse retina (blue lines). *Gnaz* and *Drd4* mRNAs were also examined in rat retina (red lines) and rat pineal gland (black lines). The mRNA levels are plotted as a function of ZT and the lines represent the periodic sinusoidal functions determined by cosinor analysis (solid and broken line for $p < 0.05$ and $p > 0.05$ in cosinor analysis). Data represent a percentage of the average value of the transcript amount during the 24-h period. Statistical analysis of transcriptional profiling is provided in Table 2. The value of ZT0 is plotted twice at both ZT0 and ZT24. The solid bars indicate the dark period. Each value represents mean ± SEM (n = 4; each n represents two retinae and a pineal gland of one animal). Note that the mRNA levels of exclusively *Gnaz* and *Drd4* exhibit significant variations in all applied settings.

https://doi.org/10.1371/journal.pone.0187411.g001

Gnai3, *Gnal*, *Gnao1*, *Gnaq*, *Gnas*) displayed a 24-h rhythm (data not shown). Similarly, rhythmic expression of Gβ subunits (*Gnb1*, *Gnb2*, *Gnb3*, *Gnb4*, *Gnb5*), and Gγ subunits (*Gngt1*, *Gngt2*) was not observed (data not shown).

Gnaz rhythmicity displayed peak expression in darkness and was similar in retina of mouse and rat (Fig 1, blue versus red lines; for statistical analysis, see Table 2). It also occurred in rat pineal gland, an organ that is phylogenetically related to the retina and is controlled by the body's master clock in the suprachiasmatic nucleus [29] (Fig 1, black lines; for statistical analysis, see Table 2). This suggests that daily regulation of *Gnaz* is phylogenetically conserved and may in retina and pineal gland be promoted by different clocks.

Daily regulation of $G\alpha_z$ protein amount

To investigate whether the observed variations in *Gnaz* mRNA result in corresponding variations in protein amount, $G\alpha_z$ immunoreactivity was compared at different ZTs in Western blot analysis by using an antibody that recognizes a band of ~ 39 kDa (Fig 2), a molecular mass in the range of the predicted size from the *Gnaz* gene (355 amino acids). The intensity of $G\alpha_z$ immunostaining tended to display a daily change ($p = 0.062$ in one-way ANOVA) with peak values around ZT21 (Fig 2). The temporal gap between the peaks in *Gnaz* mRNA (ZT16.9) and $G\alpha_z$ protein (ZT21) may reflect the time necessary to translate the transcript into protein.

Table 2. Statistical analysis of transcriptional profiling illustrated in Fig 1 and Figs 4–6.

Source of transcriptomes	*Gnaz*			*Drd4*			see Figure
	p-value	acrophase (h)	amplitude (%)	p-value	acrophase (h)	amplitude (%)	
mouse retina (C3H/f$^{+/+}$ (rd^{++})); WT; LD	< 0.05	16.9	31.9	< 0.05	19.6	46.5	Fig 1, Fig 4
rat retina (Sprague-Dawley); LD	< 0.05	18.2	40.8	< 0.05	20.1	49.9	Fig 1
rat pineal gland (Sprague-Dawley); LD	< 0.05	21.5	50.8	< 0.05	22.6	126.2	Fig 1
mouse photoreceptors (C3H/f$^{+/+}$ (rd^{++})); WT; LD	< 0.05	19.9	37.5	< 0.05	19.7	49.0	Fig 4
mouse retina (C3H/f$^{+/+}$ (rd^{++})); WT; DD	< 0.05	18.8	29.2	< 0.05	17.9	29.1	Fig 4
mouse retina (C3H/f$^{+/+}$ (rd^{++})); Clock$^{+/+}$; LD	< 0.05	16.9	31.9	< 0.05	19.6	46.5	Fig 5
mouse retina (C3H/f$^{+/+}$ (rd^{++})); Clock$^{-/-}$; LD	> 0.05	-	-	> 0.05	-	-	Fig 5
mouse retina (C3H/f$^{+/+}$ (rd^{++})); MT1$^{+/+}$-; LD	< 0.05	18.2	28.2	< 0.05	19.1	51.8	Fig 5
mouse retina (C3H/f$^{+/+}$ (rd^{++})); MT1$^{-/-}$; LD	< 0.05	16.7	33.1	< 0.05	19.0	62.5	Fig 5
mouse retina (C3H/f$^{+/+}$ (rd^{++})); Drd4$^{+/+}$; LD	< 0.05	17.9	33.8	< 0.05	18.7	47.3	Fig 5
mouse retina (C3H/f$^{+/+}$ (rd^{++})); Drd4$^{-/-}$; LD	> 0.05	-	-	n. d.	-	-	Fig 5
mouse retina (C57BL/6Jb); db/+; LD	< 0.05	18.6	11.1	< 0.05	18.5	20.1	Fig 6
mouse retina (C57BL/6Jb); db/db; LD	> 0.05	-	-	> 0.05	-	-	Fig 6

https://doi.org/10.1371/journal.pone.0187411.t002

Thus, this observation suggests that daily regulation of *Gnaz* mRNA amount causes a corresponding rhythm of Gα$_z$ protein.

Daily regulation of Gα$_z$ protein localization

Localization of Gα$_z$ protein was investigated in fluorescence microscopy (Fig 3) by conducting double labeling analysis for Gα$_z$ and centrin3, a marker of the connecting cilium and the inner

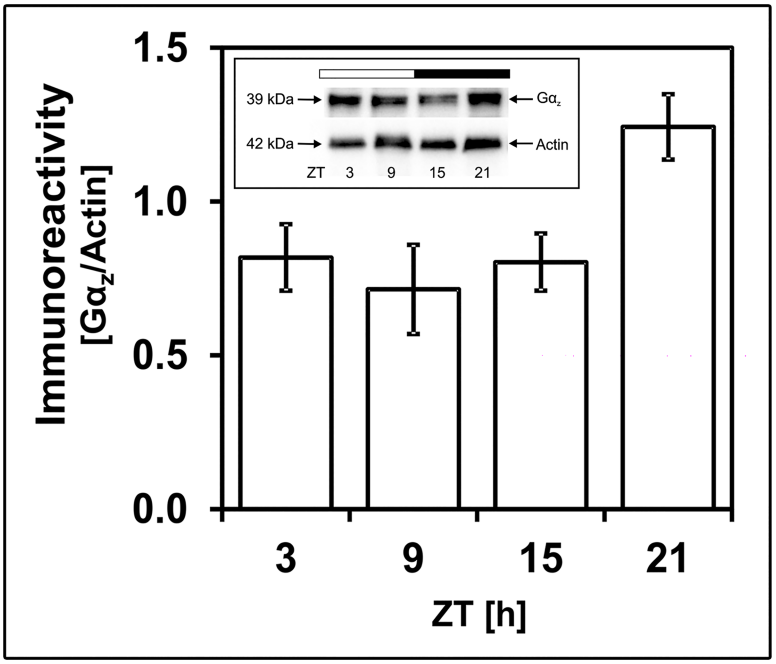

Fig 2. 24-h profiling of Gα$_z$ immunoreactivity. The figure shows a representative Western blot with Gα$_z$ immunostaining at 39 kDa and β-actin staining as a loading control. The diagram displays the quantification of Gα$_z$ immunoreactivity in relation to the corresponding β-actin signal. Data were obtained using densitometric measurement. Each value represents mean ± SEM (n = 4; each n represents two animals (four retinae)). Note that Gα$_z$ immunoreactivity tends to exhibit daily changes with peak expression around ZT21 ($p = 0.062$ in one-way ANOVA). The solid bar indicates the dark period.

https://doi.org/10.1371/journal.pone.0187411.g002

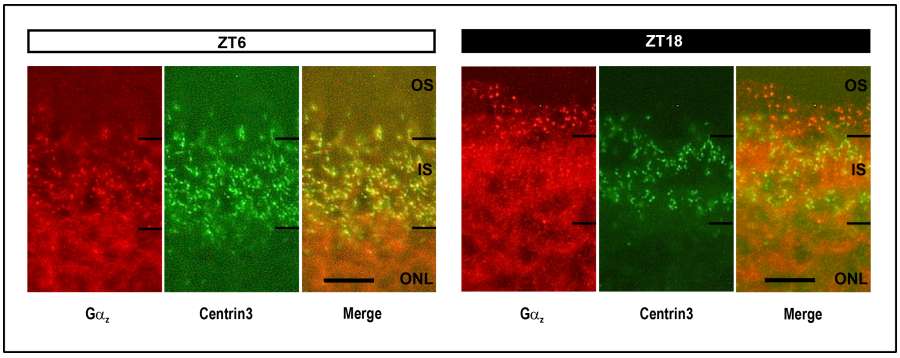

Fig 3. Daily translocation of $G\alpha_z$ immunoreactivity. Micrographs of coronal sections of the retina, labelled for $G\alpha_z$ (red) and centrin3 (green), a marker of the connecting cilium and the photoreceptor inner segment (IS). The representative immunofluorescent image shows that $G\alpha_z$ protein is abundant in photoreceptors where its subcellular localization is under daily regulation. $G\alpha_z$ immunoreactivity mainly occurs in the inner segment (IS) at ZT6 and in the outer segment (OS) at ZT18. The solid bars indicate the dark period. ONL, outer nuclear layer. Scale bar, 10 μm.

https://doi.org/10.1371/journal.pone.0187411.g003

segment of photoreceptors [30]. $G\alpha_z$ immunoreactivity mainly occurred in photoreceptors where its subcellular localization was seen to vary between day and night. This follows from the observation that $G\alpha_z$ staining mainly arose in the connecting cilium/inner segment at ZT6 and was most dense in the outer segment at ZT18 (Fig 3). This supports a concept in which subcellular localization of $G\alpha_z$ protein might exhibit a lighting condition-dependent transport from the connecting cilium/the inner segment to the outer segment.

Daily regulation of *Gnaz* mRNA amount in photoreceptor cells

The expression of *Gnaz* in photoreceptors raises the question whether rhythmicity of *Gnaz* mRNA arises from this cell type. To address this question, daily profiling of *Gnaz* mRNA was performed in photoreceptors enriched by using the LMPC technique. *Gnaz* transcript amount was seen to display a daily rhythm (Fig 4, red lines; for statistical analysis, see Table 2) with a 24-h profile resembling that obtained from preparations of the whole retina (Fig 4, blue lines;

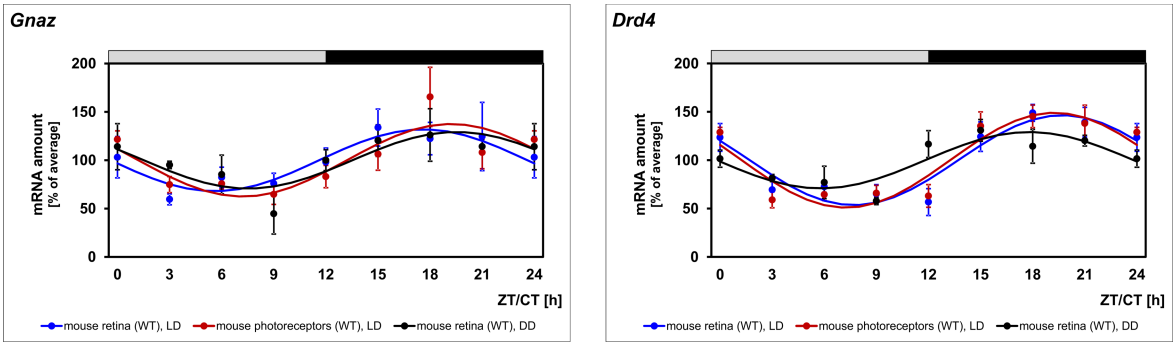

Fig 4. Daily profiling of *Gnaz* mRNA in photoreceptors and constant darkness. Transcript levels of *Gnaz* and *Drd4* were monitored under LD in mouse retina (blue lines) and mouse photoreceptors (red lines), as well as in mouse retina under DD (black lines) using qPCR. The mRNA levels are plotted as a function of ZT and circadian time (CT). The lines represent the periodic sinusoidal functions determined by cosinor analysis. Data represent a percentage of the average value of the transcript amount during the 24-h period. Statistical analysis of transcriptional profiling is provided in *Table 2*. Note that *Gnaz* mRNA rhythmicity is also evident in photoreceptors and persists in constant darkness. The value of ZT0 is plotted twice at both ZT0 and ZT24. The solid bars indicate the dark period. Each value represents mean ± SEM (n = 4; each n represents one animal (two retinae) for whole retina preparations and two animals (four retinae) for photoreceptor preparations).

https://doi.org/10.1371/journal.pone.0187411.g004

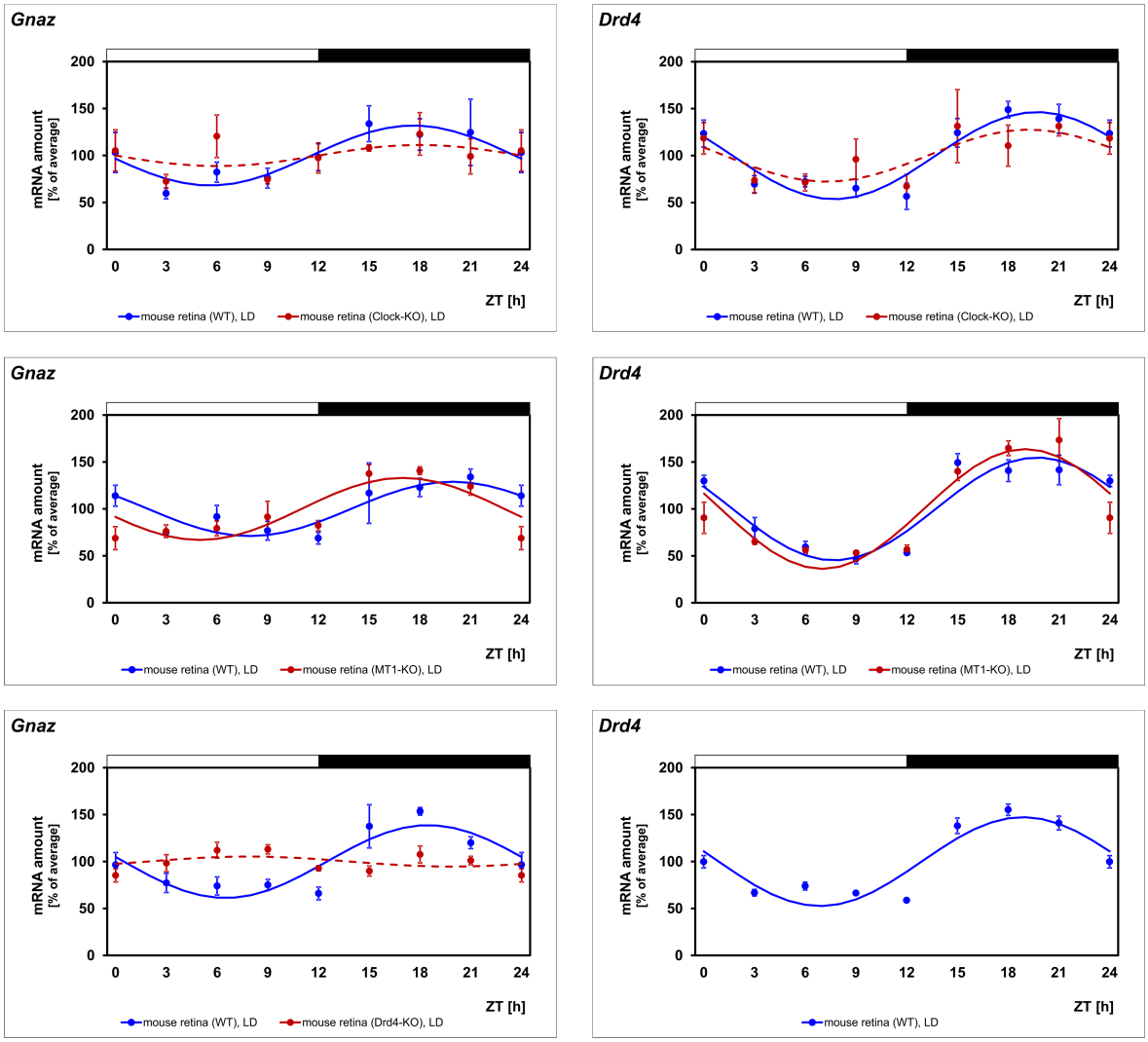

Fig 5. Daily profiling of *Gnaz* mRNA in mice deficient for *Clock*, *MT1* or *Drd4*. Transcript levels of *Gnaz* and *Drd4* were recorded in WT mice (blue lines) versus mice deficient (red lines) for *Clock* (first row), melatonin receptor type 1 (second row) or dopamine D_4 receptor (third row) in preparations of the whole retina under LD using qPCR. The mRNA levels are plotted as a function of ZT. The lines represent the periodic sinusoidal functions determined by cosinor analysis (solid and broken line for $p < 0.05$ and $p > 0.05$). Data represent a percentage of the average value of the transcript amount during the 24-h period. Statistical analysis of transcriptional profiling is provided in Table 2. Note that expression of *Gnaz* is arrhythmic in mice deficient for *Clock* or dopamine D_4 receptors and tends to be phase-advanced in mice deficient for *MT1*. The value of ZT0 is plotted twice at both ZT0 and ZT24. The solid bars indicate the dark period. Each value represents mean ± SEM (n = 4; each n represents one animal (two retinae)). *Drd4* mRNA was not detectable in *Drd4* deficient retinae.

https://doi.org/10.1371/journal.pone.0187411.g005

for statistical analysis, see Table 2). Therefore, daily changes in retinal *Gnaz* mRNA amount may partly or fully derive from photoreceptors.

Gnaz expression depends on a circadian regulator

24-h regulation of a gene may be promoted by a true circadian clock or light/dark-transitions. To test circadian regulation of *Gnaz*, 24-h profiling of transcript amount was conducted in mice adapted to DD (Fig 4, black lines; for statistical analysis, see Table 2). Consistent with clock-dependent regulation of *Gnaz* expression, the daily rhythm of *Gnaz* transcript persisted

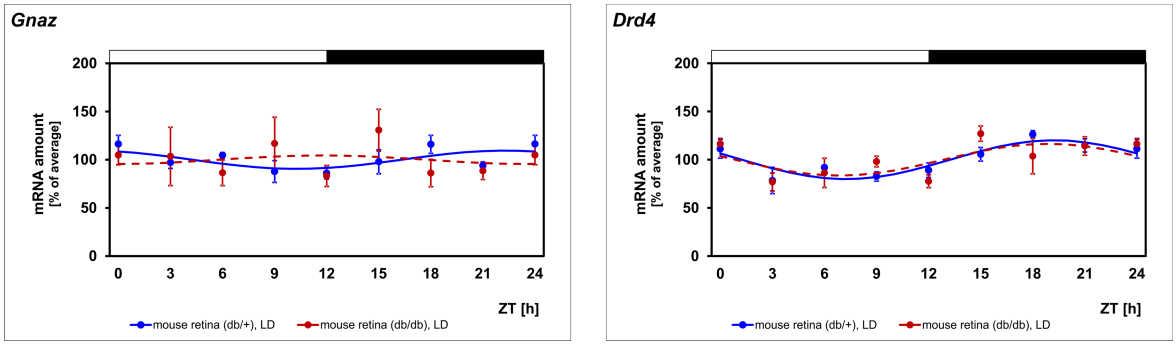

Fig 6. Daily profiling of *Gnaz* mRNA in diabetic retina. Transcript levels of *Gnaz* and *Drd4* were recorded in non-diabetic (*db/+*) mice (blue lines) versus diabetic (*db/db*) mice (red lines) in preparations of the whole retina under LD using qPCR. The mRNA levels are plotted as a function of ZT. The lines represent the periodic sinusoidal functions determined by cosinor analysis (solid and broken line for $p < 0.05$ and $p > 0.05$). Data represent a percentage of the average value of the transcript amount during the 24-h period. Statistical analysis of transcriptional profiling is provided in Table 2. Note that *Gnaz* expression is arrhythmic in diabetic mice. The value of ZT0 is plotted twice at both ZT0 and ZT24. The solid bars indicate the dark period. Each value represents mean ± SEM (n = 4; each n represents one animal (two retinae)).

https://doi.org/10.1371/journal.pone.0187411.g006

under DD. Furthermore, *Gnaz* was not rhythmically expressed in *Clock* deficient mice (Fig 5, first row, blue versus red lines; for statistical analysis, see Table 2). This supports the concept that *Gnaz* rhythmicity is driven by a retinal clock that requires *Clock* for its functionality [31] and not by the master clock in the suprachiasmatic nucleus (SCN), which does not require *Clock* for its functionality [32–34].

Circadian regulation of *Gnaz* requires dopamine D_4 receptors

In order to evaluate the contribution of melatonin and dopamine to daily regulation of *Gnaz*, 24-h profiling of the gene was performed in mice deficient for *MT1* (Fig 5, second row, blue versus red lines; for statistical analysis, see Table 2) or *Drd4* (Fig 5, third row, blue versus red lines; for statistical analysis, see Table 2). The daily rhythm of *Gnaz* was seen to persist in *MT1* deficient mice but peak expression appeared to be slightly phase-advanced. This observation suggests that melatonin signaling via MT_1 receptors does not drive rhythmicity of *Gnaz* but might influence its phasing. More importantly, daily regulation of *Gnaz* was absent in *Drd4* deficient mice. This suggests that dopamine and D_4 receptors play a role in driving circadian changes in *Gnaz* expression. In mouse retina dopamine release and D_4 receptor stimulation occurs in a circadian manner [12]. Therefore, this finding supports the concept that *Gnaz* expression depends on a clock-driven dopamine signal.

Expression of *Gnaz* is arrhythmic in diabetic retina

To test the assumption that diabetic retinopathy impairs circadian control of *Gnaz*, the *db/db* mouse, a model of Type II diabetes [35] was used. The non-diabetic phenotype (*db/+*) was seen to display a daily rhythm in *Gnaz* mRNA but with a lower amplitude than that observed in previous experiments (Fig 6, blue lines; for statistical analysis, see Table 2). This may be due to a different genetic background of the *db/db* mice (C57BL/6Jb) and the other mouse strains, which were on a C3H background. Different to the non-diabetic phenotype (*db/+*), *Gnaz* expression was arrhythmic in diabetic (*db/db*) mice (Fig 6, blue versus red lines; for statistical analysis, see Table 2). Therefore, circadian regulation of *Gnaz* appears to be disturbed in diabetic retinopathy.

Daily profiling of the clock-dependent gene *Drd4* confirms the validity of the experimental system

To test the validity of the experimental system and the obtained results, the clock-driven gene *Drd4* was monitored in the same transcriptomes as those utilized for *Gnaz* mRNA determination. Consistent with the validity of the results obtained for *Gnaz*, *Drd4* expression was observed to be rhythmic in retina of mouse and rat and pineal gland (Fig 1, for statistical analysis, see Table 2). As expected for a gene under circadian regulation, *Drd4* rhythmicity persisted under DD (Fig 4, black lines; for statistical analysis, see Table 2) and was damped in mice deficient for *Clock* (Fig 5, first row, blue versus red lines; for statistical analysis, see Table 2). Beyond what was previously known, *Drd4* rhythmicity was seen in the present study to persist in mice deficient for *MT1* (Fig 5, second row, blue versus red lines; for statistical analysis, see Table 2) and, according to statistical analysis, not in diabetic (*db/db*) mice (Table 2; Fig 6, blue versus red lines).

Discussion

The gene *Gnaz* encodes $G\alpha_z$, a unique Gi/o subfamily member, whose tissue distribution is quite restricted to primarily neuronal and endocrine tissue [36], including retina [37–39]. The findings of the present study extend previous knowledge on *Gnaz*/$G\alpha_z$ distribution [37, 40–42] by showing that it is highly expressed in photoreceptors and pinealocytes—both cell types originating phylogenetically and ontogenetically from a common ancestral cell type [29].

Gnaz mRNA—but not *Gnat1* or *Gnat2 mRNA*—displays a daily rhythm in retina. This finding and large sequence similarities of *Gnaz* with *Gnat1* and *Gnat2* (44% and 43% respectively), suggest that the earlier reported daily change in α-transducin mRNA [20–22] relies on *Gnaz* but not on the visual types of α-transducin. This assumption is furthermore supported by the fact that in transcriptomes of the murine retina, *Gnaz* displays a higher day/night change than *Gnat2* and *Gnat1* does not undergo daily regulation at all [8]. Additionally the oligodeoxynucleotide probes used previously to detect α-transducin [20] are highly complementary with all types of α-transducin (*Gnaz*: 82%, *Gnat1*: 93%, *Gnat2*: 79%).

In the context of the functional significance of the rhythmic expression of the *Gnaz* gene, it is noteworthy that daily rhythmicity is also evident at the level of $G\alpha_z$ protein. The daily profile in G*naz* mRNA resembles that in $G\alpha_z$ protein. This suggests that daily regulation of *Gnaz* mRNA evokes a corresponding rhythm in $G\alpha_z$ protein. Since $G\alpha_z$ protein expression predominates in photoreceptors (this study), but may also be abundant in the inner retina [37], *Gnaz* expression might be under daily/circadian regulation not only in photoreceptors but also in inner retinal neurons. This assumption is consistent with the observation that the acrophase of *Gnaz* expression tends to differ in microdissected photoreceptors (ZT19.9) and preparations of the whole retina (ZT16.9). Furthermore, *Gnaz*/$G\alpha_z$ is under daily regulation not only in respect to its expression but also in its subcellular localization within photoreceptors. This follows from the finding that $G\alpha_z$ immunostaining was most dense in the connecting cilium/inner segment at ZT6 but in the outer segment at ZT18. Since $G\alpha_z$ de-novo formation should occur in the inner segment, the temporary localization of $G\alpha_z$ protein in the outer segment suggests that newly synthesized $G\alpha_z$ is transported from the inner to the outer segment of photoreceptors.

Regulation of *Gnaz* expression was observed to be driven by a circadian clock. This is evident from the present observation that *Gnaz* rhythmicity persists under constant darkness and therefore does not require light/dark transitions. Circadian control of *Gnaz* appears to be driven by the retinal circadian clock system and not by the master clock in the SCN. This follows from the finding that *Gnaz* rhythmicity was not observed in *Clock*-deficient mice, in which circadian rhythms persist in the SCN due to the CLOCK homologue NPAS2 [32–34].

Rhythmicity of *Gnaz* was also evident in the pineal gland, a neuroendocrine transducer of the circadian system [43]. The pineal gland in general and its gene expression in particular are mainly under the control of the master clock in the SCN [44]. This suggests that *Gnaz* expression is circadian in both, retina and pineal gland, but in the retina depends on retinal clocks and in the pineal gland on the master clock in the SCN. The coincidence of *Gnaz* rhythmicity in mammalian photoreceptors and pinealocytes suggests that circadian regulation of *Gnaz* is evolutionary conserved. In both tissues, rhythmicity of *Gnaz* may depend on the clock-driven release of neurotransmitters. Thus circadian regulation of *Gnaz* may be mediated by dopamine in the retina (see below) and by noradrenaline in the pineal gland–the intra-pineal release of the latter neurotransmitter is known to be under the control of the SCN [45].

In murine retina, 24-h regulation of *Gnaz* appears to be mediated by dopamine signaling via D_4 receptors. This follows from the present observation that the lack of functional D_4 receptors prevents daily periodicity of *Gnaz*. Since photoreceptors combine daily rhythmicity of *Gnaz* with the occurrence of D_4 receptors [15], dopaminergic regulation of $G\alpha_z$ may mainly occur in photoreceptors. D_4 receptor-mediated regulation of photoreceptor function appears to depend on the clock-driven [46, 47] release of dopamine from amacrine cells in the inner retina [4, 48]. Therefore, circadian $G\alpha_z$ expression in photoreceptors may be driven by the clock within amacrine cells. Like *Gnaz*, the genes *Cpt-1α*, *Acadm* and *Nr4a1* have been identified to be under circadian and dopaminergic control in photoreceptors [49, 50]. Therefore, clock-dependent dopamine release from amacrine cells may be of general importance for driving rhythmicity of photoreceptor gene expression.

In contrast to D_4 receptors, MT_1 receptors do not play a role in driving rhythmicity of *Gnaz*. This follows from the present finding that notwithstanding the loss of functional MT_1 receptors 24-h changes in *Gnaz* transcript are retained. However, the removal of functional MT_1 receptors might result in advanced phasing of *Gnaz* (this study) and other genes shown to be rhythmic in photoreceptors including *Cpt-1α* and *Acadm* [50]. Therefore, melatonin acting on photoreceptor MT_1 receptors [51, 52] might influence the phasing of gene expression rhythmicity in photoreceptors. Considering that melatonin is released by photoreceptors and may feedback on photoreceptor MT_1 receptors, autocrine signaling might direct the phasing of gene rhythmicity in photoreceptors. Alternatively, melatonin might alter the phase of the clock in dopaminergic amacrine cells.

Daily rhythmicity of *Gnaz* is abolished in early diabetic retinopathy in the *db/db* mouse. Therefore, it might also be disturbed in diabetic retinopathy of humans—one of the most common causes of blindness in Europe and USA [53]. Since diabetic retinopathy affects dopamine content [54] and rhythmicity of *Drd4* expression (this study), the disturbed circadian regulation of *Gnaz* may reflect dysfunction of the retinal dopaminergic system under diabetic conditions. This assumption is consistent with the observation that circadian regulation of other genes under dopaminergic control is disturbed in diabetic retinopathy [50].

Circadian regulation of $G\alpha_z$ suggests a role of $G\alpha_z$ in linking the circadian clock to G protein-dependent signal transduction. Taken into account that $G\alpha_z$ is known to regulate adenylyl cyclase activity [55, 56], it may contribute to circadian regulation of adenylyl cyclase activity and cAMP levels in retina [16, 57]. Since $G\alpha_z$ is generally known to repress adenylyl cyclase activity, this assumption is consistent with the finding that the level of retinal $G\alpha_z$—with a peak at late night and a nadir during day (this study)—is inversely correlated with the level of cAMP—showing a nadir at late night and a peak at dusk [16].

$G\alpha_z$ has been conclusively linked to various types of GPCRs [58, 59]. Therefore, $G\alpha_z$ might link the circadian clock to GPCR-dependent signal transduction. Interestingly, in tissues other than retina $G\alpha_z$ has been shown to be coupled to D_2-like receptors [60, 61]—a subclass of dopamine receptors that includes the dopamine D_4 receptor type—and thus to a receptor

family important for vision [17, 18, 62] and healthy retinal function [54]. However, data from immunoprecipitation studies (not shown) do not support direct coupling of $G\alpha_z$ to dopamine D_4 receptors in retina.

Interestingly, $G\alpha_z$ has been seen in the SCN to be coupled to Gpr176, an orphan GPRC that sets the pace of circadian behavior [63]. This suggests a role of $G\alpha_z$ in setting the phase of the master clock in the SCN. This assumption combined with rhythmicity of *Gnaz* in retina (this study) and pineal gland (this study) indicates that $G\alpha_z$ is abundant and might play a clock-related role in all three components of the circadian system [43]. Accordingly, the α-transducin family appears to comprise clock- (*Gnaz*) and vision-related (*Gnat1*, *Gnat2*) G proteins.

In conclusion, the data of the present study suggest a concept in which $G\alpha_z$ links the circadian clock and the dopaminergic system to GPCR signaling. Future investigations using $G\alpha_z$ null mice [61, 64, 65] are warranted to reveal the exact function of $G\alpha_z$ in photoreceptors and herewith its specific functional role in photoreceptor adaptation. The present data may also provide a suitable basis for future investigations dealing with the clock-related role of $G\alpha_z$ in the circadian system.

Acknowledgments

The authors gratefully thank Ms. Ute Frederiksen, Ms. Kristina Schäfer and Dr. Tanja Wolloscheck for their excellent technical assistance, Mr. Klaus Wolloscheck for statistical advice, Ms. Susanne Rometsch and Ms. Bettina Wiechers-Schmied for secretarial help, Prof. Dr. Uwe Wolfrum for providing us with the antibody against Centrin3, and Prof. Dr. Russell G. Foster for providing us with C3H/f$^{+/+}$ (*rd*$^{++}$) mice. The data contained in this study are included in the theses of Patrick Vancura and Shaima Abdelhadi as a partial fulfillment of their doctorate degree at the Johannes Gutenberg University, Mainz.

Author Contributions

Conceptualization: Rainer Spessert.

Formal analysis: Patrick Vancura.

Funding acquisition: Gianluca Tosini, P. Michael Iuvone.

Investigation: Patrick Vancura, Shaima Abdelhadi, Erika Csicsely.

Methodology: Kenkichi Baba, Gianluca Tosini, P. Michael Iuvone, Rainer Spessert.

Project administration: Rainer Spessert.

Resources: Kenkichi Baba, Gianluca Tosini, P. Michael Iuvone.

Supervision: Rainer Spessert.

Writing – original draft: Patrick Vancura, Rainer Spessert.

Writing – review & editing: Patrick Vancura, Gianluca Tosini, P. Michael Iuvone, Rainer Spessert.

References

1. Tosini G, Menaker M. The clock in the mouse retina: melatonin synthesis and photoreceptor degeneration. Brain Res. 1998; 789(2):221–8. PMID: 9573370.
2. Kamphuis W, Cailotto C, Dijk F, Bergen A, Buijs RM. Circadian expression of clock genes and clock-controlled genes in the rat retina. Biochem Biophys Res Commun. 2005; 330(1):18–26. https://doi.org/10.1016/j.bbrc.2005.02.118 PMID: 15781226.

3. Ruan GX, Zhang DQ, Zhou T, Yamazaki S, McMahon DG. Circadian organization of the mammalian retina. Proc Natl Acad Sci U S A. 2006; 103(25):9703–8. https://doi.org/10.1073/pnas.0601940103 PMID: 16766660; PubMed Central PMCID: PMCPMC1480470.
4. Ruan GX, Allen GC, Yamazaki S, McMahon DG. An autonomous circadian clock in the inner mouse retina regulated by dopamine and GABA. PLoS Biol. 2008; 6(10):e249. https://doi.org/10.1371/journal.pbio.0060249 PMID: 18959477; PubMed Central PMCID: PMCPMC2567003.
5. Tosini G, Davidson AJ, Fukuhara C, Kasamatsu M, Castanon-Cervantes O. Localization of a circadian clock in mammalian photoreceptors. FASEB J. 2007; 21(14):3866–71. https://doi.org/10.1096/fj.07-8371com PMID: 17621597; PubMed Central PMCID: PMCPMC2385786.
6. Schneider K, Tippmann S, Spiwoks-Becker I, Holthues H, Wolloscheck T, Spatkowski G, et al. Unique clockwork in photoreceptor of rat. J Neurochem. 2010; 115(3):585–94. https://doi.org/10.1111/j.1471-4159.2010.06953.x PMID: 20722965.
7. Sandu C, Hicks D, Felder-Schmittbuhl MP. Rat photoreceptor circadian oscillator strongly relies on lighting conditions. Eur J Neurosci. 2011; 34(3):507–16. https://doi.org/10.1111/j.1460-9568.2011.07772.x PMID: 21771113.
8. Storch KF, Paz C, Signorovitch J, Raviola E, Pawlyk B, Li T, et al. Intrinsic circadian clock of the mammalian retina: importance for retinal processing of visual information. Cell. 2007; 130(4):730–41. https://doi.org/10.1016/j.cell.2007.06.045 PMID: 17719549; PubMed Central PMCID: PMCPMC2040024.
9. Cameron MA, Barnard AR, Lucas RJ. The electroretinogram as a method for studying circadian rhythms in the mammalian retina. J Genet. 2008; 87(5):459–66. PMID: 19147934.
10. Cameron MA, Barnard AR, Hut RA, Bonnefont X, van der Horst GT, Hankins MW, et al. Electroretinography of wild-type and Cry mutant mice reveals circadian tuning of photopic and mesopic retinal responses. J Biol Rhythms. 2008; 23(6):489–501. https://doi.org/10.1177/0748730408325874 PMID: 19060258.
11. Iuvone PM, Tosini G, Pozdeyev N, Haque R, Klein DC, Chaurasia SS. Circadian clocks, clock networks, arylalkylamine N-acetyltransferase, and melatonin in the retina. Prog Retin Eye Res. 2005; 24(4):433–56. https://doi.org/10.1016/j.preteyeres.2005.01.003 PMID: 15845344.
12. McMahon DG, Iuvone PM, Tosini G. Circadian organization of the mammalian retina: from gene regulation to physiology and diseases. Prog Retin Eye Res. 2014; 39:58–76. https://doi.org/10.1016/j.preteyeres.2013.12.001 PMID: 24333669; PubMed Central PMCID: PMCPMC3927986.
13. Baba K, Pozdeyev N, Mazzoni F, Contreras-Alcantara S, Liu C, Kasamatsu M, et al. Melatonin modulates visual function and cell viability in the mouse retina via the MT1 melatonin receptor. Proc Natl Acad Sci U S A. 2009; 106(35):15043–8. https://doi.org/10.1073/pnas.0904400106 PMID: 19706469; PubMed Central PMCID: PMCPMC2736407.
14. Sengupta A, Baba K, Mazzoni F, Pozdeyev NV, Strettoi E, Iuvone PM, et al. Localization of melatonin receptor 1 in mouse retina and its role in the circadian regulation of the electroretinogram and dopamine levels. PLoS One. 2011; 6(9):e24483. https://doi.org/10.1371/journal.pone.0024483 PMID: 21915336; PubMed Central PMCID: PMCPMC3168505.
15. Pozdeyev N, Tosini G, Li L, Ali F, Rozov S, Lee RH, et al. Dopamine modulates diurnal and circadian rhythms of protein phosphorylation in photoreceptor cells of mouse retina. Eur J Neurosci. 2008; 27(10):2691–700. https://doi.org/10.1111/j.1460-9568.2008.06224.x PMID: 18547251; PubMed Central PMCID: PMCPMC2440701.
16. Jackson CR, Chaurasia SS, Hwang CK, Iuvone PM. Dopamine D(4) receptor activation controls circadian timing of the adenylyl cyclase 1/cyclic AMP signaling system in mouse retina. Eur J Neurosci. 2011; 34(1):57–64. https://doi.org/10.1111/j.1460-9568.2011.07734.x PMID: 21676039; PubMed Central PMCID: PMCPMC3129439.
17. Jackson CR, Ruan GX, Aseem F, Abey J, Gamble K, Stanwood G, et al. Retinal dopamine mediates multiple dimensions of light-adapted vision. J Neurosci. 2012; 32(27):9359–68. https://doi.org/10.1523/JNEUROSCI.0711-12.2012 PMID: 22764243; PubMed Central PMCID: PMCPMC3400466.
18. Hwang CK, Chaurasia SS, Jackson CR, Chan GC, Storm DR, Iuvone PM. Circadian rhythm of contrast sensitivity is regulated by a dopamine-neuronal PAS-domain protein 2-adenylyl cyclase 1 signaling pathway in retinal ganglion cells. J Neurosci. 2013; 33(38):14989–97. https://doi.org/10.1523/JNEUROSCI.2039-13.2013 PMID: 24048828; PubMed Central PMCID: PMCPMC3776053.
19. Wettschureck N, Offermanns S. Mammalian G proteins and their cell type specific functions. Physiol Rev. 2005; 85(4):1159–204. https://doi.org/10.1152/physrev.00003.2005 PMID: 16183910.
20. Brann MR, Cohen LV. Diurnal expression of transducin mRNA and translocation of transducin in rods of rat retina. Science. 1987; 235(4788):585–7. PMID: 3101175.
21. Bowes C, van Veen T, Farber DB. Opsin, G-protein and 48-kDa protein in normal and rd mouse retinas: developmental expression of mRNAs and proteins and light/dark cycling of mRNAs. Exp Eye Res. 1988; 47(3):369–90. PMID: 2846333.

22. Sokolov M, Lyubarsky AL, Strissel KJ, Savchenko AB, Govardovskii VI, Pugh EN Jr., et al. Massive light-driven translocation of transducin between the two major compartments of rod cells: a novel mechanism of light adaptation. Neuron. 2002; 34(1):95–106. PMID: 11931744.

23. Goldmann T, Burgemeister R, Sauer U, Loeschke S, Lang DS, Branscheid D, et al. Enhanced molecular analyses by combination of the HOPE-technique and laser microdissection. Diagn Pathol. 2006; 1:2. https://doi.org/10.1186/1746-1596-1-2 PMID: 16759346; PubMed Central PMCID: PMCPMC1501060.

24. Mears AJ, Kondo M, Swain PK, Takada Y, Bush RA, Saunders TL, et al. Nrl is required for rod photoreceptor development. Nat Genet. 2001; 29(4):447–52. https://doi.org/10.1038/ng774 PMID: 11694879.

25. Osborne NN, Beaton DW, Vigny A, Neuhoff V. Localization of tyrosine-hydroxylase immunoreactive cells in rabbit retinal cultures. Neurosci Lett. 1984; 50(1–3):117–20. PMID: 6149500.

26. Kunst S, Wolloscheck T, Holter P, Wengert A, Grether M, Sticht C, et al. Transcriptional analysis of rat photoreceptor cells reveals daily regulation of genes important for visual signaling and light damage susceptibility. J Neurochem. 2013; 124(6):757–69. https://doi.org/10.1111/jnc.12089 PMID: 23145934.

27. Refinetti R, Lissen GC, Halberg F. Procedures for numerical analysis of circadian rhythms. Biol Rhythm Res. 2007; 38(4):275–325. https://doi.org/10.1080/09291010600903692 PMID: 23710111; PubMed Central PMCID: PMCPMC3663600.

28. Cornelissen G. Cosinor-based rhythmometry. Theor Biol Med Model. 2014; 11:16. https://doi.org/10.1186/1742-4682-11-16 PMID: 24725531; PubMed Central PMCID: PMCPMC3991883.

29. Rath MF, Rohde K, Klein DC, Moller M. Homeobox genes in the rodent pineal gland: roles in development and phenotype maintenance. Neurochem Res. 2013; 38(6):1100–12. https://doi.org/10.1007/s11064-012-0906-y PMID: 23076630; PubMed Central PMCID: PMCPMC3570627.

30. Trojan P, Krauss N, Choe HW, Giessl A, Pulvermuller A, Wolfrum U. Centrins in retinal photoreceptor cells: regulators in the connecting cilium. Prog Retin Eye Res. 2008; 27(3):237–59. https://doi.org/10.1016/j.preteyeres.2008.01.003 PMID: 18329314.

31. Ruan GX, Gamble KL, Risner ML, Young LA, McMahon DG. Divergent roles of clock genes in retinal and suprachiasmatic nucleus circadian oscillators. PLoS One. 2012; 7(6):e38985. https://doi.org/10.1371/journal.pone.0038985 PMID: 22701739; PubMed Central PMCID: PMCPMC3372489.

32. Debruyne JP, Noton E, Lambert CM, Maywood ES, Weaver DR, Reppert SM. A clock shock: mouse CLOCK is not required for circadian oscillator function. Neuron. 2006; 50(3):465–77. https://doi.org/10.1016/j.neuron.2006.03.041 PMID: 16675400.

33. Debruyne JP. Oscillating perceptions: the ups and downs of the CLOCK protein in the mouse circadian system. J Genet. 2008; 87(5):437–46. PMID: 19147932; PubMed Central PMCID: PMCPMC2749070.

34. DeBruyne JP, Weaver DR, Reppert SM. CLOCK and NPAS2 have overlapping roles in the suprachiasmatic circadian clock. Nat Neurosci. 2007; 10(5):543–5. https://doi.org/10.1038/nn1884 PMID: 17417633; PubMed Central PMCID: PMCPMC2782643.

35. Yang Q, Xu Y, Xie P, Cheng H, Song Q, Su T, et al. Retinal Neurodegeneration in db/db Mice at the Early Period of Diabetes. J Ophthalmol. 2015; 2015:757412. https://doi.org/10.1155/2015/757412 PMID: 25821591; PubMed Central PMCID: PMCPMC4363796.

36. Ho MK, Wong YH. G(z) signaling: emerging divergence from G(i) signaling. Oncogene. 2001; 20(13):1615–25. https://doi.org/10.1038/sj.onc.1204190 PMID: 11313909.

37. Hinton DR, Blanks JC, Fong HK, Casey PJ, Hildebrandt E, Simons MI. Novel localization of a G protein, Gz-alpha, in neurons of brain and retina. J Neurosci. 1990; 10(8):2763–70. PMID: 2117645.

38. Hollborn M, Ulbricht E, Rillich K, Dukic-Stefanovic S, Wurm A, Wagner L, et al. The human Muller cell line MIO-M1 expresses opsins. Mol Vis. 2011; 17:2738–50. PMID: 22065927; PubMed Central PMCID: PMCPMC3209432.

39. Jiang M, Pandey S, Tran VT, Fong HK. Guanine nucleotide-binding regulatory proteins in retinal pigment epithelial cells. Proc Natl Acad Sci U S A. 1991; 88(9):3907–11. PMID: 1902575; PubMed Central PMCID: PMCPMC51562.

40. Fong HK, Yoshimoto KK, Eversole-Cire P, Simon MI. Identification of a GTP-binding protein alpha subunit that lacks an apparent ADP-ribosylation site for pertussis toxin. Proc Natl Acad Sci U S A. 1988; 85(9):3066–70. PMID: 3129724; PubMed Central PMCID: PMCPMC280144.

41. Matsuoka M, Itoh H, Kozasa T, Kaziro Y. Sequence analysis of cDNA and genomic DNA for a putative pertussis toxin-insensitive guanine nucleotide-binding regulatory protein alpha subunit. Proc Natl Acad Sci U S A. 1988; 85(15):5384–8. PMID: 2456569; PubMed Central PMCID: PMCPMC281761.

42. Blatt C, Eversole-Cire P, Cohn VH, Zollman S, Fournier RE, Mohandas LT, et al. Chromosomal localization of genes encoding guanine nucleotide-binding protein subunits in mouse and human. Proc Natl Acad Sci U S A. 1988; 85(20):7642–6. PMID: 2902634; PubMed Central PMCID: PMCPMC282248.

43. Hastings MH, Maywood ES, Reddy AB. Two decades of circadian time. J Neuroendocrinol. 2008; 20(6):812–9. https://doi.org/10.1111/j.1365-2826.2008.01715.x PMID: 18601704.

44. Bailey MJ, Coon SL, Carter DA, Humphries A, Kim JS, Shi Q, et al. Night/day changes in pineal expression of >600 genes: central role of adrenergic/cAMP signaling. J Biol Chem. 2009; 284(12):7606–22. https://doi.org/10.1074/jbc.M808394200 PMID: 19103603; PubMed Central PMCID: PMCPMC2658055.

45. Maronde E, Stehle JH. The mammalian pineal gland: known facts, unknown facets. Trends Endocrinol Metab. 2007; 18(4):142–9. https://doi.org/10.1016/j.tem.2007.03.001 PMID: 17374488.

46. Gustincich S, Contini M, Gariboldi M, Puopolo M, Kadota K, Bono H, et al. Gene discovery in genetically labeled single dopaminergic neurons of the retina. Proc Natl Acad Sci U S A. 2004; 101(14):5069–74. https://doi.org/10.1073/pnas.0400913101 PMID: 15047890; PubMed Central PMCID: PMCPMC387375.

47. Dorenbos R, Contini M, Hirasawa H, Gustincich S, Raviola E. Expression of circadian clock genes in retinal dopaminergic cells. Vis Neurosci. 2007; 24(4):573–80. https://doi.org/10.1017/S0952523807070538 PMID: 17705893.

48. Witkovsky P. Dopamine and retinal function. Doc Ophthalmol. 2004; 108(1):17–40. PMID: 15104164.

49. Kunst S, Wolloscheck T, Kelleher DK, Wolfrum U, Sargsyan SA, Iuvone PM, et al. Pgc-1alpha and Nr4a1 Are Target Genes of Circadian Melatonin and Dopamine Release in Murine Retina. Invest Ophthalmol Vis Sci. 2015; 56(10):6084–94. https://doi.org/10.1167/iovs.15-17503 PMID: 26393668; PubMed Central PMCID: PMCPMC4585341.

50. Vancura P, Wolloscheck T, Baba K, Tosini G, Iuvone PM, Spessert R. Circadian and Dopaminergic Regulation of Fatty Acid Oxidation Pathway Genes in Retina and Photoreceptor Cells. PLoS One. 2016; 11(10):e0164665. https://doi.org/10.1371/journal.pone.0164665 PMID: 27727308; PubMed Central PMCID: PMCPMC5058478.

51. Savaskan E, Wirz-Justice A, Olivieri G, Pache M, Krauchi K, Brydon L, et al. Distribution of melatonin MT1 receptor immunoreactivity in human retina. J Histochem Cytochem. 2002; 50(4):519–26. https://doi.org/10.1177/002215540205000408 PMID: 11897804.

52. Baba K, Benleulmi-Chaachoua A, Journe AS, Kamal M, Guillaume JL, Dussaud S, et al. Heteromeric MT1/MT2 melatonin receptors modulate photoreceptor function. Sci Signal. 2013; 6(296):ra89. https://doi.org/10.1126/scisignal.2004302 PMID: 24106342; PubMed Central PMCID: PMCPMC3867265.

53. Stitt AW, Lois N, Medina RJ, Adamson P, Curtis TM. Advances in our understanding of diabetic retinopathy. Clin Sci (Lond). 2013; 125(1):1–17. https://doi.org/10.1042/CS20120588 PMID: 23485060.

54. Aung MH, Park HN, Han MK, Obertone TS, Abey J, Aseem F, et al. Dopamine deficiency contributes to early visual dysfunction in a rodent model of type 1 diabetes. J Neurosci. 2014; 34(3):726–36. https://doi.org/10.1523/JNEUROSCI.3483-13.2014 PMID: 24431431; PubMed Central PMCID: PMCPMC3891954.

55. Yang J, Wu J, Jiang H, Mortensen R, Austin S, Manning DR, et al. Signaling through Gi family members in platelets. Redundancy and specificity in the regulation of adenylyl cyclase and other effectors. J Biol Chem. 2002; 277(48):46035–42. https://doi.org/10.1074/jbc.M208519200 PMID: 12297509.

56. Kimple ME, Joseph JW, Bailey CL, Fueger PT, Hendry IA, Newgard CB, et al. Galphaz negatively regulates insulin secretion and glucose clearance. J Biol Chem. 2008; 283(8):4560–7. https://doi.org/10.1074/jbc.M706481200 PMID: 18096703.

57. Fukuhara C, Liu C, Ivanova TN, Chan GC, Storm DR, Iuvone PM, et al. Gating of the cAMP signaling cascade and melatonin synthesis by the circadian clock in mammalian retina. J Neurosci. 2004; 24(8):1803–11. Epub 2004/02/27. https://doi.org/10.1523/JNEUROSCI.4988-03.2004 PMID: 14985420.

58. Sanchez-Blazquez P, Rodriguez-Munoz M, de la Torre-Madrid E, Garzon J. Brain-specific Galphaz interacts with Src tyrosine kinase to regulate Mu-opioid receptor-NMDAR signaling pathway. Cell Signal. 2009; 21(9):1444–54. https://doi.org/10.1016/j.cellsig.2009.05.003 PMID: 19446022.

59. Chan AS, Lai FP, Lo RK, Voyno-Yasenetskaya TA, Stanbridge EJ, Wong YH. Melatonin mt1 and MT2 receptors stimulate c-Jun N-terminal kinase via pertussis toxin-sensitive and -insensitive G proteins. Cell Signal. 2002; 14(3):249–57. PMID: 11812653

60. Leck KJ, Blaha CD, Matthaei KI, Forster GL, Holgate J, Hendry IA. Gz proteins are functionally coupled to dopamine D2-like receptors in vivo. Neuropharmacology. 2006; 51(3):597–605. https://doi.org/10.1016/j.neuropharm.2006.05.002 PMID: 16814816.

61. van den Buuse M, Martin S, Brosda J, Leck KJ, Matthaei KI, Hendry I. Enhanced effect of dopaminergic stimulation on prepulse inhibition in mice deficient in the alpha subunit of G(z). Psychopharmacology (Berl). 2005; 183(3):358–67. https://doi.org/10.1007/s00213-005-0181-6 PMID: 16220329.

62. Nir I, Harrison JM, Haque R, Low MJ, Grandy DK, Rubinstein M, et al. Dysfunctional light-evoked regulation of cAMP in photoreceptors and abnormal retinal adaptation in mice lacking dopamine D4 receptors. J Neurosci. 2002; 22(6):2063–73. PMID: 11896146.

63. Doi M, Murai I, Kunisue S, Setsu G, Uchio N, Tanaka R, et al. Gpr176 is a Gz-linked orphan G-protein-coupled receptor that sets the pace of circadian behaviour. Nat Commun. 2016; 7:10583. https://doi.org/10.1038/ncomms10583 PMID: 26882873; PubMed Central PMCID: PMCPMC4757782.

64. Kimple ME, Moss JB, Brar HK, Rosa TC, Truchan NA, Pasker RL, et al. Deletion of GalphaZ protein protects against diet-induced glucose intolerance via expansion of beta-cell mass. J Biol Chem. 2012; 287(24):20344–55. https://doi.org/10.1074/jbc.M112.359745 PMID: 22457354; PubMed Central PMCID: PMCPMC3370216.

65. Hultman R, Kumari U, Michel N, Casey PJ. Galphaz regulates BDNF-induction of axon growth in cortical neurons. Mol Cell Neurosci. 2014; 58:53–61. https://doi.org/10.1016/j.mcn.2013.12.004 PMID: 24321455; PubMed Central PMCID: PMCPMC4096435.